

Evaluation of maturation competence of metaphase II oocytes in mice based on the distance between pericentriolar materials of meiotic spindle

Distance of PCM during oocyte maturation

Chizuka Sakai · Yumi Hoshino · Yusuke Sato · Eimei Sato

Received: 21 July 2010 / Accepted: 13 October 2010 / Published online: 17 November 2010
© Springer Science+Business Media, LLC 2010

Abstract

Purpose To ascertain whether metaphase II (MII) spindle shape influences oocyte competence, we examined the meiotic spindle organization in in vivo ovulated (IVO) oocytes and in spontaneously matured or follicle stimulating hormone (FSH)-induced oocytes.

Methods FSH-induced oocytes matured in Waymouth's MB752/1 or human tubal fluid (HTF) media and oocytes matured spontaneously in the basal medium were obtained, and spindles were detected by immunofluorescence. To evaluate the fertilization-associated differences in spindle morphology, we performed in vitro fertilization and analysed integrin mRNA expression.

Results The distance between the pericentriolar materials (PCMs) in oocytes matured under all conditions was initially more, but it reduced gradually and increased again thereafter. Therefore, oocytes exhibiting a reduction in the distance between PCMs had the highest development rate to blastocyst in each condition.

Conclusion These results indicate that the 'maturation competence' of MII oocytes can be evaluated on the basis of the distance between PCMs.

Keywords In vitro maturation · Maturation competence · Meiotic spindle · Mouse oocyte · Pericentriolar materials

Introduction

In vitro meiotic resumption, which is characterized by germinal vesicle breakdown (GVBD), is either a spontaneous or a gonadotropin-induced response. The former occurs as a consequence of oocyte removal from the inhibitory environment of the follicle [1], while the latter is induced by gonadotropin action on cumulus cells that produce meiosis-inducing signals capable of overriding meiotic arrest [2–4]. In both the processes, a key step is the decrease in intracellular cyclic adenosine monophosphate (cAMP) levels [5, 6] and the subsequent activation of the M-phase promoting factor (MPF) and the mitogen-activated protein kinase (MAPK) pathway [3]. Follicle stimulating hormone (FSH) induces complete meiotic maturation, i.e., first polar body (PB1) emission, of cultured cumulus-oocyte complexes (COCs). Hypoxanthine maintains meiotic arrest in cultured COCs, while FSH reverses this inhibitory effect of hypoxanthine [2].

In vitro maturation (IVM) has been efficiently used to obtain metaphase II (MII)-arrested mouse oocytes that are competent to be fertilized and are capable of producing viable embryos [7, 8]. The developmental competence of in vitro matured (IVM) oocytes of mammals is likely to be inferior to that of in vivo matured oocytes [9–12]. After it was reported that mammalian oocytes can spontaneously resume and complete meiosis upon removal from the follicle [1, 13], much effort has been expended to modify the culture conditions of IVM in order to obtain high-quality oocytes for embryo production [14, 15]. In some mammals, such as cattle, IVM represents the industry standard and is routinely used for in vitro fertilization or nuclear transfer and embryo production strategies, and this method affords relatively high rates of blastocyst development and implantation [16, 17]. Although live young

Capsule The 'maturation competence' of MII oocytes can be evaluated on the basis of the distance between pericentriolar materials (PCMs) of spindles.

C. Sakai (✉) · Y. Hoshino · Y. Sato · E. Sato
Laboratory of Animal Reproduction,
Graduate School of Agricultural Science, Tohoku University,
Sendai 981-8555, Japan
e-mail: chizuka@bios.tohoku.ac.jp

individuals have been successfully produced from IVM oocytes of some mammals, including humans, the distinguishing features of *in vivo* ovulated (IVO) oocytes, which confer a high developmental potential to these oocytes, remain obscure [18]. From a practical point of view, to optimize IVM, it is necessary to achieve successful embryonic development and identify oocyte markers that predict successful nuclear and cytoplasmic maturation.

In oocytes, the meiotic spindle plays an important role in chromosome alignment and separation during meiosis. Typically, meiotic spindles of mouse oocytes are anastral; however, the degree of spindle pole tapering and minus end focusing varies widely between species [19] and with the conditions under which meiotic maturation occurs [20]. Significant differences have been observed between IVO and IVM oocytes of mice with regard to meiotic spindle shape and size. IVO oocytes exhibit spindles with a focused pole, whereas IVM oocytes typically display large barrel-shaped anastral spindles that appear more pronounced after different treatments [20, 21]. The significance of deviations in the meiotic spindle shape and size with respect to the quality of oocytes has not been fully investigated.

We aimed to identify the maturation conditions under which the shape of the spindle in IVM oocytes was similar to that of the spindle in IVO MII oocytes and to increase the maturation competence of IVM oocytes. To this end, we cultured mouse oocytes in the germinal-vesicle (GV) stage

under different conditions and evaluated the relationship between spindle shape and ‘maturation competence’.

Materials and methods

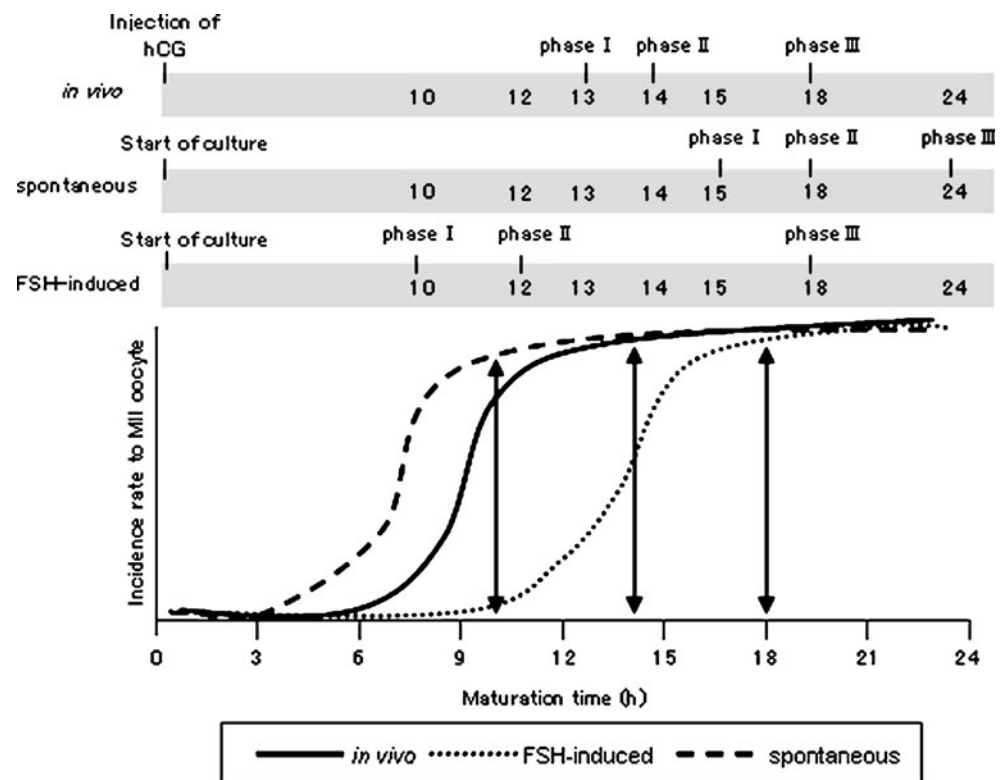
Animals

ICR mice were purchased from Japan SLC Inc. (Shizuoka) and bred in our laboratory. Immature 20- to 23-day-old mice were used for all experiments. The experimental procedures described in this report were performed in accordance with the Guide for the Care and Use of Laboratory Animals published by Tohoku University.

Collection of oocytes matured *in vivo* and *in vitro*

The maturation time under each maturation condition was divided into phase I, II, and III (Fig. 1); phase I was immediately after PB1 emission, phase II was the common maturation time, and phase III was the prolonged maturation time after PB1 emission. To obtain *in vivo* oocytes, we first primed the mice with 5 IU of pregnant mare’s serum gonadotropin (PMSG) (Teikoku Hormone MFG, Tokyo) and then with 5 IU of human chorionic gonadotropin (hCG) (Teikoku Hormone MFG) after 48 h. At 13 (phase I), 14 (phase II), and 18 h (phase III) after hCG treatment, MII-

Fig. 1 General timeline of maturation in mice. Phase I, II, and III in *in vivo* matured oocytes are 13, 14, and 18 h, respectively. Phase I, II, and III in spontaneously matured oocytes are 10, 12, and 18 h, respectively. Phase I, II, and III in FSH-induced matured oocytes are 15, 18, and 24 h, respectively. The arrows indicate the maturation time reached incidence rate to MII oocyte plateau (phase I)



arrested oocytes released from the oviductal ampullae were collected in Leibovitz's L-15 medium (Invitrogen, Grand Island, NY) containing 0.1% polyvinyl alcohol (PVA) (Sigma, St. Louis, MO) and 4 mM hypoxanthine (Sigma). The cumulus cells were removed by treatment with 0.1% hyaluronidase at room temperature. *In vitro* oocyte maturation was induced according to previously described methods [22]. The COCs were isolated from mice at 48 h after PMSG injection by puncturing the large antral follicles with a 26-gauge needle and were collected in Leibovitz's L-15 medium containing 0.1% PVA and 4 mM hypoxanthine in order to maintain the oocytes in the GV-stage. For spontaneous meiotic maturation experiments of COCs, we used the following culture media: Waymouth's MB752/1 medium (Invitrogen) or human tubal fluid (HTF) medium (Irvine Scientific, Santa Ana, CA) containing 5% fetal calf serum (FCS) (Gemini Bio, CA), 0.23 mM pyruvic acid (Sigma), 75 mg/l penicillin G (Meiji Seika, Tokyo), and 50 mg/l streptomycin sulphate (Meiji Seika). These media were designed as the basal media. To evaluate FSH-induced meiotic maturation, we added 4 mM hypoxanthine and 100 IU/l FSH (Sigma) to the basal media. The COCs were cultured in 100 μ l droplets of the culture medium overlaid with paraffin liquid (Nacalai Tesque, Kyoto) in a humidified atmosphere of 5% CO₂ in air at 37°C for 10 (phase I), 12 (phase II), and 18 h (phase III) (basal medium) or for 15 (phase I), 18 (phase II), and 24 h (phase III) (FSH-induced medium). At the end of culture, oocytes were removed from the cumulus cells by treatment with 0.1% hyaluronidase at room temperature.

Immunodetection of microtubules and pericentrin in mouse oocytes

Immunolocalization in oocytes was performed according to previously described methods [22]. Oocytes were washed three times in phosphate-buffered saline (PBS, Nissui, Tokyo) containing 0.1% PVA (PBS-PVA), and denuded oocytes were fixed with 2% paraformaldehyde (Sigma) in Dulbecco's PBS(-) containing 0.1% PVA and 0.2% Triton X-100 at room temperature for 60 min. Microtubules were detected by using anti- α -tubulin (Sigma; 1:500) and Alexa Fluor 488-labelled goat anti-mouse IgG antibodies (Invitrogen; 1:200). Pericentriolar materials (PCMs) were detected by using anti-pericentrin (BD biosciences, NJ; 1:100) and Alexa Fluor 488-labelled goat anti-mouse IgG antibodies. The chromosomes were labelled with 10 μ g/ml propidium iodide (Sigma), and oocytes were viewed using a Bio-Rad MRC-1024 confocal scanning laser microscope mounted on an Axioplan Zeiss microscope. Confocal images shown in the Results are representative of at least 30 oocytes matured under each maturation condition and obtained from more than five animals.

Quantification of spindle size

Digital images were obtained from MII oocytes with a Bio-Rad MRC-1024 confocal scanning laser microscope mounted on an Axioplan Zeiss microscope, and spatial measurements were recorded with Motic Images Plus 2.0S (Shimadzu, Kyoto). The central plane of the spindle was defined as the region with the largest spindle area in which the distance between 2 points of PCMs was the maximum. Only digital images in which spindle boundaries were clearly defined and the spindles were oriented properly were used to obtain measurements of spindle area, oocyte area, distance between PCMs and chromosome width; from these values, the relative spindle area and distance between PCMs of meiotic spindle were calculated for each oocyte.

In vitro fertilization and embryo culture

In vitro fertilization and embryo culture were performed according to the previously described methods [22]. Spermatozoa were collected from the cauda epididymis and preincubated for 2–3 h in 400 μ l of HTF medium to allow capacitation before insemination. After capacitation, the spermatozoa were introduced into 200 μ l droplets of the fertilization medium at a final concentration of 700 spermatozoa/ μ l. At 4 h after insemination, the penetration of sperms into the oocytes was confirmed by microscopic examination; subsequently, the oocytes were washed thoroughly 5 times and then cultured in the KSOM medium. All embryos were incubated in 100 μ l droplets of culture medium in a humidified atmosphere of 5% CO₂ in air at 37°C.

Reverse transcriptase-polymerase chain reaction

We collected 20 MII oocytes matured under each maturation condition; total RNA was extracted and cDNA synthesis was performed by using Cells-to-cDNA™ II (Ambion, Austin, TX). Polymerase chain reaction (PCR) was performed using Ex Taq polymerase (TaKaRa, Shiga). Each primer was designed as described in the previous reports [22, 23]. For integrin α 6, the sense (5'-GAGGAA-TATCCAAACTGAACTAC-3') and antisense (5'-GGAATGCTGTCATCGTACCTAGAG-3') primers generated a 398-bp fragment. For integrin β 1, the sense (5'-GTGACCCATTGCAAGGAGAAGGA-3') and antisense primers (5'-GTCATGAATTATCATTAAAAGT TTCCA-3') generated a 217-bp fragment. For glyceraldehyde-3-phosphate dehydrogenase (G3PDH), the sense (5'-CCACTCTTCCACCTTCGATG-3') and antisense primers (5'-GAGGGAGATGCTCAGTGTTG-3') generated a 226-bp fragment. The amplification conditions were as follows: 94°C for 10 min; 35 cycles of 30 s each

of denaturation at 94°C, annealing at 52°C for integrin $\alpha 6$, 52°C for integrin $\beta 1$, and 57°C for G3PDH, and extension at 72°C; and a final extension for 10 min at 72°C. The DNA Data Bank of Japan/European Molecular Biology Laboratory/GenBank accession numbers for integrin $\alpha 6$, integrin $\beta 1$, and G3PDH cDNA sequences are X69902, Y00769, and M32599, respectively.

Statistical analysis

There were at least three replicates for each experiment. Data were expressed as the mean \pm SD and analysed using ANOVA, followed by Bonferroni's protective least significant difference test ($P < 0.05$). The statistical significance was evaluated by using STATVIEW (Abacus Concepts Inc., Berkeley, CA).

Results

Comparison of spindle size in in vivo- and in vitro-matured MII oocytes

The spindle size in oocytes matured under the three maturation conditions was analysed by immunostaining and digital imaging. The representative images of oocytes

from each treatment group are shown in Fig. 2. Oocytes matured in vivo contained small spindles (Fig. 2A–C). MII oocytes matured in vitro spontaneously cultured in Waymouth's MB752/1 medium typically contained large and barrel-shaped spindles (Fig. 2D–F). MII oocytes matured in FSH-induced Waymouth's MB752/1 medium exhibited small spindles, similar to those of in vivo oocytes (Fig. 2G–I).

To determine whether the culture medium influenced spindle shape, we next examined the GV-stage oocytes cultured in FSH-induced Waymouth's MB752/1 medium and HTF medium (Fig. 3). Oocytes matured in FSH-induced HTF medium contained larger spindles than those matured in Waymouth's MB752/1 medium. These variations in the in vitro and in vivo matured oocytes with respect to spindle size prompted a morphometric analysis of each experimental group.

We measured the area covered by MII spindle in individual oocytes from each treatment group using Motic Images Plus 2.0S. The results are shown in Fig. 4. The results indicated that the spindle areas of MII oocytes matured in vitro spontaneously were greater than those of in vivo oocytes, whereas the areas of MII oocytes matured in FSH-induced Waymouth's MB752/1 medium were relatively similar to those of in vivo oocytes. However, the spindle areas of MII oocytes matured in FSH-induced HTF

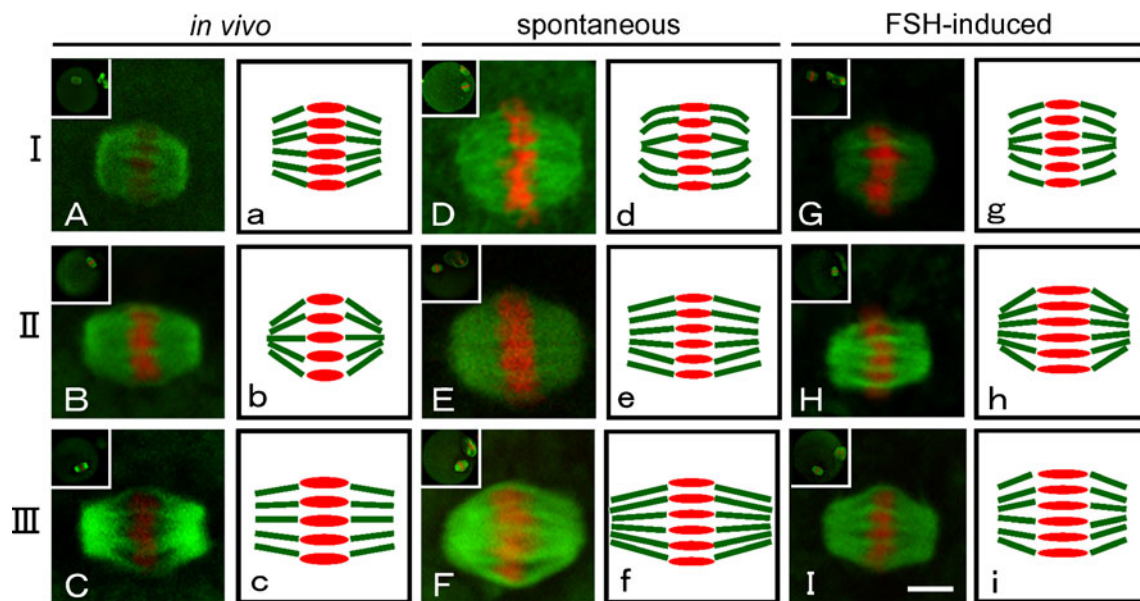


Fig. 2 Representative spindle images of in vivo (A–C, a–c), spontaneous (D–F, d–f), and FSH-induced matured (G–I, g–i) oocytes probed for microtubules (green) and chromosomes (red). The (A, a), (B, b), and (C, c) panels illustrate the 13 h (phase I), 14 h (phase II), and 18 h (phase III) hCG-treated MII oocytes matured in vivo, respectively. The (D, d), (E, e), and (F, f) panels illustrate spontaneously matured oocytes cultured for 10 h (phase I), 12 h

(phase II), and 18 h (phase III), respectively. The (G, g), (H, h), and (I, i) panels illustrate FSH-induced matured oocytes cultured for 15 h (phase I), 18 h (phase II), and 24 h (phase III), respectively. Small letters represent morphological models of spindles in oocytes matured in each maturation condition. In morphological models, green and red lines represent microtubules and chromosomes, respectively. Bar, 10 μ m

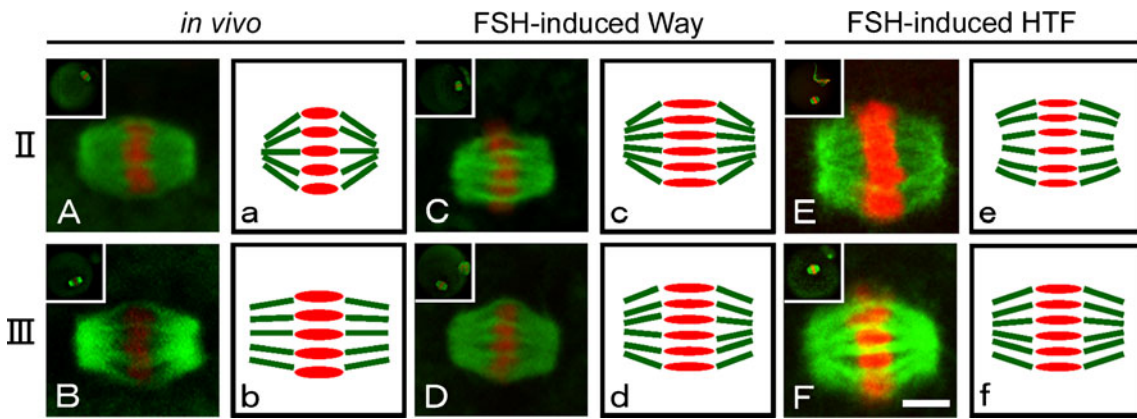


Fig. 3 Representative spindle images of in vivo oocytes (A, B, a, b) and FSH-induced matured oocytes cultured in Waymouth's MB752/1 medium (C, D, c, d) or HTF medium (E, F, e, f) probed for microtubules (green) and chromosomes (red). The (A, a) and (B, b) panels illustrate the 14 h (phase II) and 18 h (phase III) hCG-treated MII oocytes matured in vivo respectively. The (C, E, c, e) and (D, F, d,

f) panels illustrate FSH-induced matured oocytes cultured for 18 h (phase II) and 24 h (phase III), respectively. Small letters represent morphological models of spindles in oocytes matured in each maturation condition. In morphological models, green and red lines represent microtubules and chromosomes, respectively. Bar, 10 μm. Way, Waymouth's MB752/1 medium; HTF, HTF medium

medium were significantly larger than those in in vivo oocytes and oocytes matured in Waymouth's MB752/1 medium. These results suggest that although the culture medium influenced spindle size of mouse MII oocytes, MII oocytes matured in FSH-induced Waymouth's MB752/1 medium may exhibit similar spindle size as that observed in in vivo oocytes. Therefore, we used Waymouth's MB752/1 medium as the IVM culture medium in all the subsequent experiments.

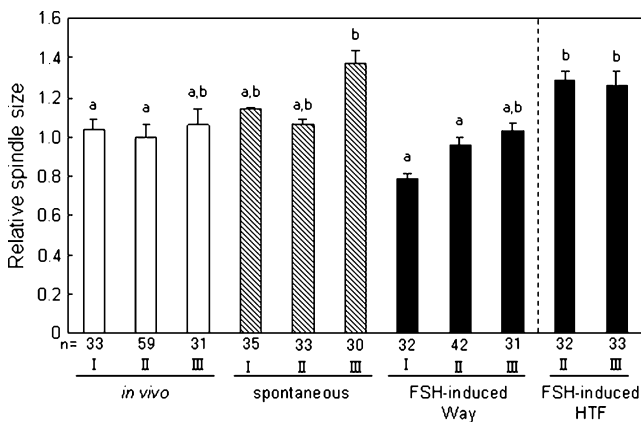


Fig. 4 The effect of different culture conditions on the size of spindle. Each bar shows in vivo (white), spontaneous (gray), and FSH-induced oocytes matured in Waymouth's MB752/1 medium or HTF medium (black). Relative spindle area indicates the mean value of spindle area/oocyte area. The total number of oocytes analysed (n) for each maturation condition are indicated at the bottom of the columns. The value of spindle size relative to that of in vivo MII oocytes (14 h after hCG injection) is indicated. Values are expressed as mean ± SD. Bars with different superscripts (a or b) are significantly different ($P < 0.05$). Way, Waymouth's MB752/1 medium; HTF, HTF medium

Localization of pericentriolar materials in in vivo- and in vitro-matured MII oocytes

Next, we determined if PCMs influenced spindle morphology. We analysed the PCMs of spindles in oocytes matured under the three maturation conditions by immunostaining and digital imaging. The representative images of oocytes from each treatment group are shown in Fig. 5. The distance between the 2 points of PCMs in MII oocytes matured under all maturation conditions was initially more (phase I); however, this distance reduced with time (phase II) and increased again thereafter (phase III). These results prompted a morphometric analysis in each experimental group.

We measured the distance between the PCMs of spindle in individual oocytes from each treatment group using Motic Images Plus 2.0S. The results are shown in Fig. 6. The distance between the PCMs of spindles in MII oocytes matured in vitro spontaneously was more and that between the PCMs of spindles in MII oocytes matured in FSH-induced Waymouth's MB752/1 medium was less than that in in vivo MII oocytes. This result indicates a trend that the distance between the PCMs in MII oocytes matured under all maturation conditions was initially more; however, this distance reduced gradually and increased again thereafter. These results suggested that the distance between the PCMs in MII oocytes may be affected by maturation conditions and time.

Differences in spindle morphologies of MII oocytes influence fertilization

To determine whether the difference in spindle morphology in MII oocytes is associated with fertilization, we per-

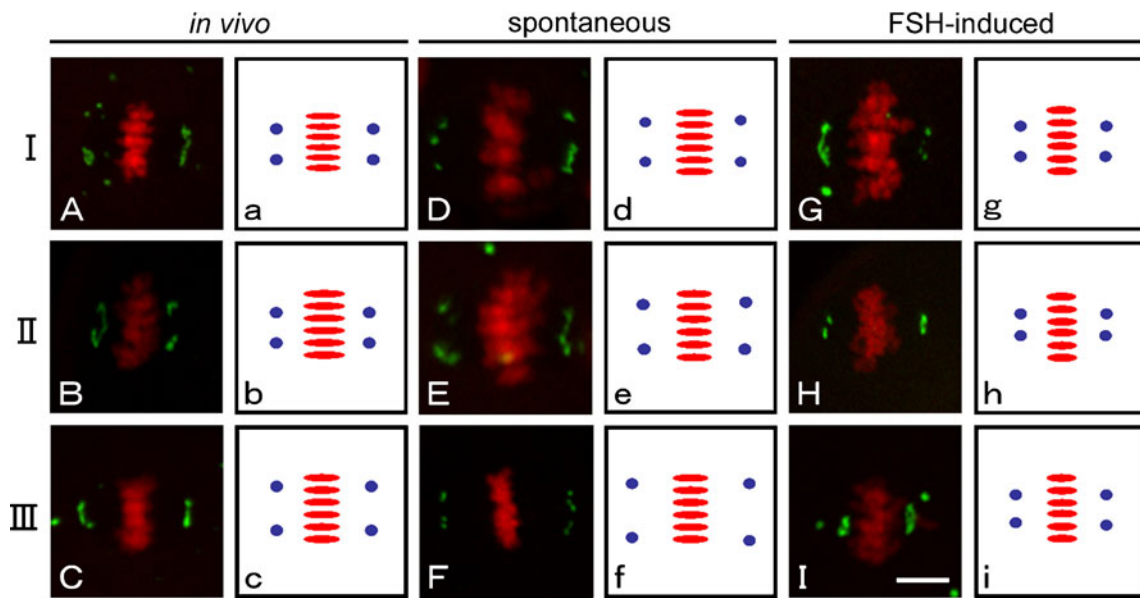


Fig. 5 Representative spindle images of *in vivo* (A–C, a–c), spontaneous (D–F, d–f), and FSH-induced matured (G–I, g–i) oocytes probed for PCMs (*green*) and chromosomes (*red*). The (A, a), (B, b), and (C, c) panels illustrate 13 h (phase I), 14 h (phase II), and 18 h (phase III) hCG-treated MII oocytes matured *in vivo*, respectively. The (D, d), (E, e), and (F, f) panels illustrate spontaneous matured oocytes cultured for 10 h (phase I), 12 h (phase II), and 18 h (phase III),

respectively. The (G, g), (H, h), and (I, i) panels illustrate FSH-induced matured oocytes cultured for 15 h (phase I), 18 h (phase II), and 24 h (phase III), respectively. Small letters represent morphological models of spindles in oocytes matured in each maturation condition. In morphological models, red lines and blue dots represent chromosomes and PCMs, respectively. Bar, 10 μ m

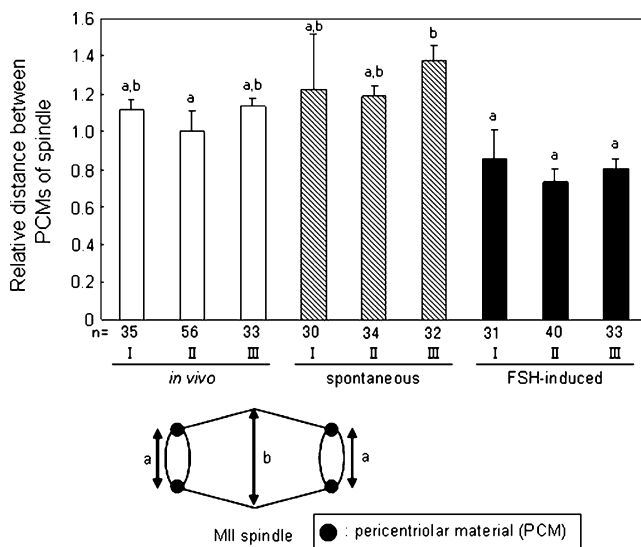


Fig. 6 Morphometric measurement of meiotic spindle under different culture conditions. Each bar shows *in vivo* (*white*), spontaneous (*gray*), and FSH-induced (*black*) groups. Values are individual distance between PCMs of meiotic spindle (distance between PCMs (a)/chromosome width (b)). The value of distance between PCMs relative to that of *in vivo* MII oocytes (14 h after hCG injection) is indicated. The total number of oocytes analysed (n) for each maturation condition are indicated at the bottom of the columns. Values are expressed as mean \pm SD. Bars with different superscripts (a or b) are significantly different ($P < 0.05$)

formed *in vitro* fertilization using mature MII oocytes that were matured under all maturation conditions. As illustrated in Table 1, the sperm penetration rate, pronuclear formation rate, and development rate to 2-cell embryos did not differ with the maturation conditions. The rate of development to blastocyst was the highest (62.7%) in MII IVO oocytes isolated 14 h after hCG treatment under all maturation conditions, and it was the second highest (60.7%) in MII oocytes matured for 18 h in FSH-induced medium.

Moreover, when MII oocytes cultured in each of the three culture conditions were examined closely, the oocytes in which the distance between PCMs was reduced (Figs. 5 and 6, phase II) exhibited the highest development rate to blastocyst in all culture conditions. This result suggests that reduction in the distance between PCMs in MII oocytes (phase II) improved their maturation competence.

To investigate this hypothesis, we examined the expression of integrins $\alpha 6$ and $\beta 1$ mRNA in MII oocytes under all maturation conditions. Oocyte integrins are essential for fertilization. In particular, integrins $\alpha 6$ and $\beta 1$ on the egg plasma membrane serve as mammalian sperm receptors and are related to fertility [24]. As shown in Fig. 7, high levels of integrins $\alpha 6$ and $\beta 1$ were detected in MII oocytes exhibiting high development rate to blastocyst in *in vitro* fertilization. These results suggested that integrins $\alpha 6$ and $\beta 1$ influence the fertility of MII oocytes, and with reducing distance between PCMs (phase II), high levels of integrins $\alpha 6$ and $\beta 1$ were detected in MII oocytes.

Table 1 Effects of culture conditions on MII oocytes and embryonic development

Maturation conditions	Phase (h)	Total number of oocytes	Sperm penetration (% ± SD) ^d	Pronuclei (% ± SD) ^d	2-cell embryos (% ± SD) ^e	Blastocyst (% ± SD) ^e	
In vivo	I (13)	161	84.9±7.7	77.7±7.8	98.8±1.2	57.3±6.9 ^a	
	II (14)	191	87.8±6.6	78.6±4.3	99.5±0.5	62.5±10.8 ^a	
	III (18)	91	99.0±1.0	87.0±6.4	99.0±1.0	19.4±7.8 ^{b,c}	
In vitro	Spontaneous	I (10)	135	92.1±4.0	63.9±3.6	93.1±5.0	13.4±5.2 ^{b,c}
		II (12)	120	88.7±4.8	85.7±3.4	82.7±4.5	36.2±5.2 ^b
		III (18)	78	90.0±3.6	84.9±4.1	89.0±6.5	25.9±2.9 ^{b,c}
	FSH-induced	I (15)	75	94.7±0.5	79.0±13.8	89.7±5.2	17.7±3.3 ^c
		II (18)	102	98.0±2.0	91.5±4.4	98.9±1.1	60.7±7.6 ^a
		III (24)	77	93.9±6.1	76.7±12.3	79.2±10.1	13.8±5.9 ^{b,c}

Values are expressed as mean ± SD. ^{a-c} Values with different superscripts within each column are significantly different ($P < 0.05$; ANOVA). No differences were observed in sperm penetration rate, pronuclear formation rate, and the development rate to two-cell embryos. ^d Values per MII oocyte; ^e Values per pronuclei

Discussion

Oocyte quality profoundly affects monospermic fertilization, early embryonic survival, maintenance of pregnancy, and even fetal development. Therefore, it is important to identify reliable indicators of oocyte quality for efficient embryo production and infertility treatment. Determination of oocyte quality by morphological assessment is a relatively popular method because it is noninvasive and convenient. Meiotic spindle morphology provides important information for predicting the developmental competence of oocytes [25]. The length of the MII spindle has been correlated with the quality of human oocytes [26, 27]. Sanfins et al. (2003) examined the spindle behaviour in naturally ovulated oocytes, IVO oocytes obtained from standard superovulation protocols, and COCs undergoing spontaneous meiotic maturation. They found that while the MII stage IVO oocytes had normal bipolar spindles with focused poles, which were characterized by the presence of distinct γ -tubulin foci, the IVM oocytes exhibited barrel-shaped spindles with few acetylated microtubules and

diffuse distribution of γ -tubulin in the microtubules. Similarly, we observed significant differences between the spindle morphologies of oocytes matured under different conditions: the spindles in IVO oocytes and oocytes matured in FSH-induced medium were small and pointed as compared to the spindles in oocytes that were spontaneously matured in vitro, as previously observed by Sanfins et al. (2003). Interestingly, the spindle morphologies in spontaneously matured oocytes are similar to those in the *Mos*^{-/-} strains of mutant oocytes [4, 28, 29]. The *Mos*^{-/-} strains of mutant oocytes have hypertrophied spindles. Moreover, *Mos*^{-/-} strains of mutant COCs cannot undergo cumulus expansion, which occurs during in vivo maturation and ovulation. Therefore, it is noteworthy that the addition of FSH to culture medium induces the partial reversion of spontaneously matured oocytes to the IVO phenotype, suggesting that COC integrity and hormone-regulated expansion play pivotal roles in microtubule patterning during oocyte maturation.

However, we compared spindle morphologies in IVO oocytes to those in oocytes matured in the 2 FSH-induced

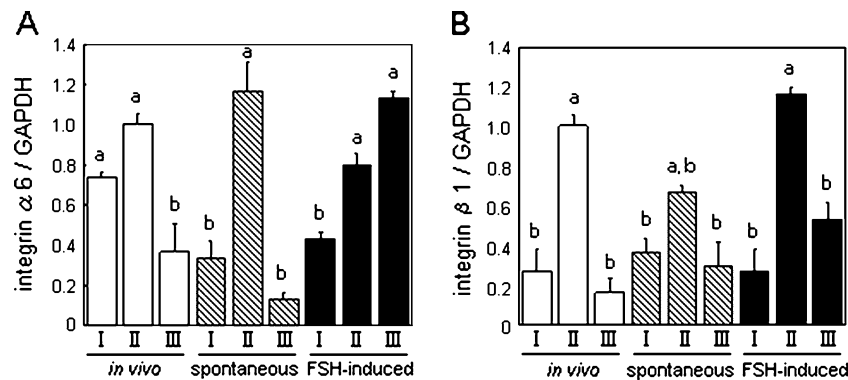


Fig. 7 RT-PCR analysis of integrin $\alpha 6$ (A) and $\beta 1$ (B) mRNA expression in different culture conditions. G3PDH was amplified as an intrinsic control. The experiments were repeated three times and similar

results were obtained. Values are expressed as mean ± SD. Bars with different superscripts (a or b) are significantly different ($P < 0.05$)

culture media (HTF and Waymouth's MB752/1 medium); the spindle areas of MII oocytes matured in FSH-induced HTF medium were significantly greater than those of IVO oocytes and oocytes matured in the Waymouth's MB752/1 medium. This result was consistent with the results of previous studies [30, 31]. These reports suggested that spindles in IVM oocytes exhibited a variation in shape from tapering poles (IVO oocytes) to large barrel shape (oocytes matured in basal medium); further, the shape of spindles in IVM oocytes cultured in supplemented medium was similar to that of IVO oocytes. Therefore, culture conditions may influence the processes underlying spindle morphogenesis, and some degree of caution is warranted in attributing significance to spindle shape variations when comparing in vivo and in vitro maturation.

In somatic cells, the centrosome is a crucial organelle for the assembly of mitotic spindles during cell division. However, centrosomes do not always contain centrioles. Although MII spindles in mouse oocytes possess centrosomal material at both meiotic poles, which is formed by the assembly of multiple small asters, the centrioles are absent. Nevertheless, this centrosomal material performs the functions that are typical of microtubule organizing centres (MTOCs) and can therefore 'qualify' as a centrosome [32]. Vertebrate oocytes contain acentriolar MTOCs in place of centrosomes, which are involved in spindle assembly (acentrosomal spindle assembly), and these MTOCs contain the PCM components, namely, γ -tubulin [33, 34] and pericentrin [35]. MII oocytes of the pig [36], sheep [37], and cow [38] do not contain cytoplasmic MTOCs, whereas those of mice contain cytoplasmic MTOCs. In mice, the acentrosomal materials containing PCMs at both meiotic spindle and cytoplasmic MTOCs are regulated to aid spindle assembly during meiotic progression [39–42]. However, it has been proposed that the barrel-shaped spindles observed in *Mos*^{-/-} strains of mutant and spontaneously matured oocytes are formed by the incorporation of an excessive number of MTOCs in the spindle [20, 40, 43, 44]. In our study, the distance between the PCMs at the spindle poles in MII oocytes matured in vitro spontaneously in all phases was more and that in MII oocytes matured in FSH-induced Waymouth's MB752/1 medium was less than that in the IVO oocytes. If spindle-associated MTOCs were limited in number or mass during spindle morphogenesis, then smaller and pointed spindles in oocytes would be expected, as observed in MII oocytes matured in FSH-induced Waymouth's MB752/1 medium and in IVO oocytes. Moreover, in our experiments, the rate of development to blastocyst was the highest in MII IVO oocytes isolated at 14 h after hCG treatment and the second highest in MII oocytes matured for 18 h in FSH-induced medium; however, the rate of development to blastocyst in MII oocytes matured spontaneously for 12 h was signifi-

cantly lower than that in the abovementioned two conditions (Table 1). After fertilization, these MTOCs function as centres for microtubule nucleation, and they participate in pronuclear movement and in the formation of subsequent mitotic spindles [45, 46]. Therefore, an abnormal reduction of cytoplasmic MTOCs could significantly reduce the oocyte competence to sustain normal embryonic development.

Our study showed that the distance between PCMs at the spindle poles in MII oocytes matured under all maturation conditions was initially more (phase I); however, this distance reduced gradually (phase II) and increased again thereafter (phase III) (Fig. 5). Further, MII oocytes with less distance between PCMs (phase II) exhibited the highest development rate to blastocyst in each MII oocyte maturation condition (Table 1). In addition, MII oocytes with high integrin $\alpha 6$ and $\beta 1$ mRNA expressions developed to the blastocyst stage (Fig. 7). We speculate that the dynamic change in PCMs and the association between the distance between PCMs and fertility influence spindle assembly and maintain spindle configuration. The pig meiotic spindle is formed by bundling of microtubules by the Nuclear Mitotic Apparatus (NuMA), which is a kind of centrosomal material, whereas the mouse meiotic spindle is formed through the gathering of cytoplasmic MTOCs [32]. First, the perinuclear acentrosomal materials containing PCMs formed multiple spindle poles. The continued activity of motor proteins, such as dynein or Ncd, would promote PCMs clustering, explaining the fusion of several small poles into large ones containing 2 PCMs clusters, and this process continued until the formation of two dominant spindles [47]. In this bipolar configuration, microtubules are stably aligned due to motor activities and chromosome biorientation, indicating that microtubule kinetochore contacts have been established [47]. We expected that the metaphase spindle morphology in phase I (immediately after PB1 emission) could be on the way of PCMs clustering at each spindle poles; therefore, the distance between 2 points of PCMs at each pole was more and the oocytes could not undergo fertilization. In phase II, this bipolar configuration could be stabilized, thereby reducing the distance between 2 points of PCMs and affording maturation competence to the oocytes. However, it has been reported that metaphase spindle in over-matured oocytes exhibit characteristic patterns of centrosome deterioration and frequently display tri- or multipolar spindle poles; these oocytes could not be fertilized, or alternatively, the fertilized oocytes exhibited aneuploidy or developmental abnormalities [48, 49]. It has been shown that MAPK activities gradually decrease in aging oocytes. MAPK is a signalling molecule associated with centrosome components [50], and the former is thought to be involved in centrosome and microtubule stabilization. Therefore, in

aging oocytes, the decrease in MAPK activities may account for centrosome and microtubule destabilization, thereby influencing fertility.

Meiotic spindle is crucial for accurate chromosomal alignment and segregation during meiosis. It is important to coordinate microtubule remodelling with the functions of cell cycle components during oocyte meiosis to achieve balanced nuclear and cytoplasmic maturation [43]. Therefore, the characteristics of the spindle, including its area, and the distance between PCMs, can be used to evaluate oocyte quality [25].

Our results suggest that oocytes exhibiting reduction in the distance between PCMs have a higher embryo developmental potential than the oocytes that exhibit increasing distance between PCMs. Conventionally, the spindles were imaged mainly by confocal microscopy analysis, which requires cell fixation and has a fatal effect on the oocyte. Alternatively, meiotic spindles can be observed directly [51] by using a polarization microscope (Polscope, Cambridge, MA). At present, the results of morphometric evaluation of the spindle obtained by using a Polscope are not consistent with those obtained by confocal analysis [52]; therefore, the distance between PCMs in metaphase spindle could not be measured using the Polscope. However, more advanced polarized light microscopy devices (e.g., the Oosight) may provide a better representation of the spindle constitution. Therefore, in the future, careful analysis of the distance between PCMs of spindle in the MII oocytes using these devices may serve as a noninvasive and reliable method of assessing oocyte quality and embryonic competence.

The findings of our study draw specific attention to the determinants of oocyte quality that influences the production of superior quality animals, preservation of endangered animals, and application of assisted-reproductive technology, and reinforces the mounting concerns over the widespread use of in vitro maturation for clinical purposes.

Acknowledgements This work was supported by the Japan Society for the Promotion of Science Grant to E. Sato (No. 21248032). This work was also supported in part by Grant-in-Aid for Young Scientists (B) to Y. Hoshino (No. 21780250) from the Ministry of Education, Science, and Culture, Japan.

References

- Pincus G, Enzmann V. The comparative behavior of mammalian eggs in vivo and in vitro. *J Exp Med*. 1935;62:655–75.
- Downs SM, Daniel SA, Eppig JJ. Induction of maturation in cumulus cell-enclosed mouse oocytes by follicle-stimulating hormone and epidermal growth factor: evidence for a positive stimulus of somatic cell origin. *J Exp Zool*. 1988;245:86–96.
- Fan HY, Sun QY. Involvement of mitogen-activated protein kinase cascade during oocyte maturation and fertilization in mammals. *Biol Reprod*. 2004;70:535–47.
- Su YQ, Wigglesworth K, Pendola FL, O'Brien MJ, Eppig JJ. Mitogen-activated protein kinase activity in cumulus cells is essential for gonadotropin-induced oocyte meiotic resumption and cumulus expansion in the mouse. *Endocrinology*. 2002;143:2221–32.
- Dekel N, Galiani D, Sherizly I. Dissociation between the inhibitory and the stimulatory action of cAMP on maturation of rat oocytes. *Mol Cell Endocrinol*. 1988;56:115–21.
- Horner K, Livera G, Hinckley M, Trinh K, Storm D, Conti M. Rodent oocytes express an active adenylyl cyclase required for meiotic arrest. *Dev Biol*. 2003;258:385–96.
- Albertini DF, Sanfins A, Combelles CM. Origins and manifestations of oocyte maturation competencies. *Reprod Biomed Online*. 2003;6:410–5.
- Wassarman PM, Jovine L, Qi H, Williams Z, Darie C, Litscher ES. Recent aspects of mammalian fertilization research. *Mol Cell Endocrinol*. 2005;234:95–103.
- Eppig JJ, O'Brien MJ. Comparison of preimplantation developmental competence after mouse oocyte growth and development in vitro and in vivo. *Theriogenology*. 1998;49:415–22.
- Mermillod P, Oussaid B, Cognie Y. Aspects of follicular and oocyte maturation that affect the developmental potential of embryos. *J Reprod Fertil Suppl*. 1999;54:449–60.
- Moor R, Dai Y. Maturation of pig oocytes in vivo and in vitro. *Reprod Suppl*. 2001;58:91–104.
- Trounson A, Anderiesz C, Jones G. Maturation of human oocytes in vitro and their developmental competence. *Reproduction*. 2001;121:51–75.
- Edwards RG. Maturation in vitro of mouse, sheep, cow, pig, rhesus monkey and human ovarian oocytes. *Nature*. 1965;208:349–51.
- Sutton ML, Gilchrist RB, Thompson JG. Effects of in-vivo and in-vitro environments on the metabolism of the cumulus-oocyte complex and its influence on oocyte developmental capacity. *Hum Reprod Update*. 2003;9:35–48.
- Telfer EE. In vitro models for oocyte development. *Theriogenology*. 1998;49:451–60.
- Barnes F, Endebrock M, Looney C, Powell R, Westhusin M, Bondioli K. Embryo cloning in cattle: the use of in vitro matured oocytes. *J Reprod Fertil*. 1993;97:317–20.
- Bousquet D, Twagiramungu H, Morin N, Brisson C, Carboneau G, Durocher J. In vitro embryo production in the cow: an effective alternative to the conventional embryo production approach. *Theriogenology*. 1999;51:59–70.
- De Rycke M, Liebaers I, Van Steirteghem A. Epigenetic risks related to assisted reproductive technologies: risk analysis and epigenetic inheritance. *Hum Reprod*. 2002;17:2487–94.
- Albertini DF, Barrett SL. The developmental origins of mammalian oocyte polarity. *Semin Cell Dev Biol*. 2004;15:599–606.
- Sanfins A, Lee GY, Plancha CE, Overstrom EW, Albertini DF. Distinctions in meiotic spindle structure and assembly during in vitro and in vivo maturation of mouse oocytes. *Biol Reprod*. 2003;69:2059–67.
- Combelles CM, Carabatsos MJ, London SN, Mailhes JB, Albertini DF. Centrosome-specific perturbations during in vitro maturation of mouse oocytes exposed to cocaine. *Exp Cell Res*. 2000;260:116–26.
- Hoshino Y, Sato E. Protein kinase B (PKB/Akt) is required for the completion of meiosis in mouse oocytes. *Dev Biol*. 2008;314:215–23.
- Sutherland AE, Calarco PG, Damsky CH. Developmental regulation of integrin expression at the time of implantation in the mouse embryo. *Development*. 1993;119:1175–86.

24. Almeida EA, Huovila AP, Sutherland AE, Stephens LE, Calarco PG, Shaw LM, et al. Mouse egg integrin alpha 6 beta 1 functions as a sperm receptor. *Cell*. 1995;81:1095–104.
25. Wang Q, Sun QY. Evaluation of oocyte quality: morphological, cellular and molecular predictors. *Reprod Fertil Dev*. 2007;19:1–12.
26. Wang WH, Meng L, Hackett RJ, Odenbourg R, Keefe DL. The spindle observation and its relationship with fertilization after intracytoplasmic sperm injection in living human oocytes. *Fertil Steril*. 2001;75:348–53.
27. Coticchio G, Sereni E, Serrao L, Mazzone S, Iadarola I, Borini A. What criteria for the definition of oocyte quality? *Ann NY Acad Sci*. 2004;1034:132–44.
28. Choi T, Fukasawa K, Zhou R, Tessarollo L, Borrer K, Resau J, et al. The Mos/mitogen-activated protein kinase (MAPK) pathway regulates the size and degradation of the first polar body in maturing mouse oocytes. *Proc Natl Acad Sci USA*. 1996;93:7032–5.
29. Choi T, Rulong S, Resau J, Fukasawa K, Matten W, Kuriyama R, et al. Mos/mitogen-activated protein kinase can induce early meiotic phenotypes in the absence of maturation-promoting factor: a novel system for analyzing spindle formation during meiosis I. *Proc Natl Acad Sci USA*. 1996;93:4730–5.
30. Barrett SL, Albertini DF. Allocation of gamma-tubulin between oocyte cortex and meiotic spindle influences asymmetric cytokinesis in the mouse oocyte. *Biol Reprod*. 2007;76:949–57.
31. Ibanez E, Sanfins A, Combelles CM, Overstrom EW, Albertini DF. Genetic strain variations in the metaphase-II phenotype of mouse oocytes matured in vivo or in vitro. *Reproduction*. 2005;130:845–55.
32. Schatten H, Sun QY. The functional significance of centrosomes in mammalian meiosis, fertilization, development, nuclear transfer, and stem cell differentiation. *Environ Mol Mutagen*. 2009;50:620–36.
33. Gueth-Hallonet C, Antony C, Aghion J, Santa-Maria A, Lajoie-Mazenc I, Wright M, et al. Gamma-Tubulin is present in acenriolar MTOCs during early mouse development. *J Cell Sci*. 1993;105(Pt 1):157–66.
34. Palacios MJ, Joshi HC, Simerly C, Schatten G. Gamma-tubulin reorganization during mouse fertilization and early development. *J Cell Sci*. 1993;104(Pt 2):383–9.
35. Carabatsos MJ, Combelles CM, Messinger SM, Albertini DF. Sorting and reorganization of centrosomes during oocyte maturation in the mouse. *Microsc Res Tech*. 2000;49:435–44.
36. Kim NH, Funahashi H, Prather RS, Schatten G, Day BN. Microtubule and microfilament dynamics in porcine oocytes during meiotic maturation. *Mol Reprod Dev*. 1996;43:248–55.
37. Le Guen P, Crozet N. Microtubule and centrosome distribution during sheep fertilization. *Eur J Cell Biol*. 1989;48:239–49.
38. Long CR, Pinto-Correia C, Duby RT, Ponce de Leon FA, Boland MP, Roche JF, et al. Chromatin and microtubule morphology during the first cell cycle in bovine zygotes. *Mol Reprod Dev*. 1993;36:23–32.
39. Calarco PG. Centrosome precursors in the acenriolar mouse oocyte. *Microsc Res Tech*. 2000;49:428–34.
40. Combelles CM, Albertini DF. Microtubule patterning during meiotic maturation in mouse oocytes is determined by cell cycle-specific sorting and redistribution of gamma-tubulin. *Dev Biol*. 2001;239:281–94.
41. Messinger SM, Albertini DF. Centrosome and microtubule dynamics during meiotic progression in the mouse oocyte. *J Cell Sci*. 1991;100(Pt 2):289–98.
42. Van Blerkom J. Microtubule mediation of cytoplasmic and nuclear maturation during the early stages of resumed meiosis in cultured mouse oocytes. *Proc Natl Acad Sci USA*. 1991;88:5031–5.
43. Sanfins A, Plancha CE, Overstrom EW, Albertini DF. Meiotic spindle morphogenesis in in vivo and in vitro matured mouse oocytes: insights into the relationship between nuclear and cytoplasmic quality. *Hum Reprod*. 2004;19:2889–99.
44. Plancha CE, Sanfins A, Rodrigues P, Albertini D. Cell polarity during folliculogenesis and oogenesis. *Reprod Biomed Online*. 2005;10:478–84.
45. Maro B, Howlett SK, Webb M. Non-spindle microtubule organizing centers in metaphase II-arrested mouse oocytes. *J Cell Biol*. 1985;101:1665–72.
46. Schatten H, Schatten G, Mazia D, Balczon R, Simerly C. Behavior of centrosomes during fertilization and cell division in mouse oocytes and in sea urchin eggs. *Proc Natl Acad Sci USA*. 1986;83:105–9.
47. Schuh M, Ellenberg J. Self-organization of MTOCs replaces centrosome function during acenriolar spindle assembly in live mouse oocytes. *Cell*. 2007;130:484–98.
48. Miao YL, Kikuchi K, Sun QY, Schatten H. Oocyte aging: cellular and molecular changes, developmental potential and reversal possibility. *Hum Reprod Update*. 2009;15:573–85.
49. Miao YL, Sun QY, Zhang X, Zhao JG, Zhao MT, Spate L, et al. Centrosome abnormalities during porcine oocyte aging. *Environ Mol Mutagen*. 2009;50:666–71.
50. Sun QY, Schatten H. Regulation of dynamic events by microfilaments during oocyte maturation and fertilization. *Reproduction*. 2006;131:193–205.
51. Wang WH, Meng L, Hackett RJ, Keefe DL. Developmental ability of human oocytes with or without birefringent spindles imaged by Polscope before insemination. *Hum Reprod*. 2001;16:1464–8.
52. Coticchio G, Sciajno R, Hutt K, Bromfield J, Borini A, Albertini DF. Comparative analysis of the metaphase II spindle of human oocytes through polarized light and high-performance confocal microscopy. *Fertil Steril*. 2010;93:2056–64.